Article

Ultrasensitive electrochemiluminescence detection of microRNA via one-step introduction of target-triggered branched hybridization chain reaction circuit

Yang Li, Cheng Zhi Huang, and Yuan Fang Li

Anal. Chem., **Just Accepted Manuscript** • DOI: 10.1021/acs.analchem.9b02580 • Publication Date (Web): 16 Jun 2019

Ultrasensitive electrochemiluminescence detection of microRNA via one-step introduction of target-triggered branched hybridization chain reaction circuit

Yang Li, † Cheng Zhi Huang*, ‡ and Yuan Fang Li*, †

† College of School of Chemistry and Chemical Engineering, Southwest University, Chongqing 400715, China.

‡ College of Pharmaceutical Science, Southwest University, Chongqing 400716, China.

* Corresponding authors: chengzhi@swu.edu.cn (C. Z. Huang); liyf@swu.edu.cn (Y. F. Li)

ABSTRACT: High sensitivity and accuracy are two key issues that evaluation the elctrochemiluminescence (ECL) detection, especially for the low-abundance nucleic acid detection. However, researches on construction of biosensor are mainly through step-by-step approach which will increase the systematic error affecting the accuracy of the detection. Here we proposed a novel strategy that introduction of branched hybridization chain reaction (bHCR) circuit to the terbium (II) organic gels (TOGs) modified electrode in one step to achieve both sensitive detection and simplified modification steps. The sensitivity of the biosensor was elevated by the cascade bHCR circuit that was activated by miRNA-141 and operated like a molecular machine to form hyperbranched DNA nanostructures. Benefiting from molecular programming, the obtained nanostructures carried a large number of dopamine molecules, which can effectively quench the ECL signal of emitters and achieve a low limit of detection (0.18 fM). Impressively, the proposed one-step approach was almost the easiest way to modify nucleic acids to electrodes. In this way, the introduction of a large molecular weight DNA structure in one step avoided the errors that may result from the stepwise modification of small molecular weight nucleic sequences into the electrode. Considering the accessible operation, favorable performance and high universality of this strategy, this work may be inspired to analyze other microRNAs and further clinical diagnosis.

KEY WORDS： electrochemiluminescence, hybridization chain reaction, accuracy, detection.

INTRODUCTION

MicroRNAs (miRNAs) are small non-coding RNA molecule that play a role in RNA gene expression and post-transcriptional regulation of gene expression.[1,2] As key components of gene expression regulation, miRNAs are directly related to diverse cancers, possessing great potential to become a new branch of biomarkers in early tumor diagnosis.[3,4] However, due to the ultralow abundance, short sequences, and high degree of sequence similarity of miRNAs, detection of miRNAs are extremely challenging.[5] Thus, many works have been focused on developing a variety of analytical techniques to achieve sensitive detection of miRNAs, such as fluorescence,[6,7] colorimetric,[8] surface-enhanced Raman scattering (SERS),[9] electrochemical,[10,11] electrochemiluminescence,[12,13] etc. Among these methods, electrochemiluminescence (ECL) is such an ideal technique to detect nucleic acid in virtue of its simple instrumentation, low background interference, high sensitivity, and wide linear ranges.[14] On the other hand, to enhance the sensitivity and pull down the limit of detection in the nucleic acid detection applications, a series of cyclic amplification strategies have been developed, including rolling circle amplification (RCA)[15,16], catalyzed hairpin assembly (CHA)[17,18], loop-mediated isothermal amplification (LAMP)[19,20] and hybridization chain reaction (HCR)[21-23]. Especially, the hybridization chain reaction (HCR), a well-known amplification strategy that the formed nicked polymeric nanowires was initiated by the triggered sequence, has shown to be as sensitive as the classical polymerase chain reaction (PCR) without

enzymes.[24] Moreover, with the development of molecular programming, diverse nucleic acid reaction circuits have been proposed on the basis of HCR to form branched and dendritic nanostructures.[25] Strikingly, the isothermal entropy-driven catalysis circuit was regard as a promising methods due to the enzyme-free and exclusive entropy-driven force.[26] Thus, applying this strategy to construct a biosensor for detecting the concentration of nucleic acids, can circumvent the need for enzyme and achieve the purpose of multiple amplification and ultrasensitive detection.

Although many signal amplification approaches have been proposed to achieve satisfying sensitivity, the importance of accuracy seems to be neglected when building biosensors. According to the current reports, no matter whether it is a simple or complicated DNA circulation strategy, almost more than one step of nucleic acid modification on the electrode is required without exception.[27,28] However, as we all known, the electrochemical reaction on the electrode is an interfacial reaction. That's to say, if too many steps are needed when constructing biosensors, more systematic errors are inevitably caused, especially for low-abundance nucleic acid detection. An interesting way to solve this problem is to assemble these nucleic acids into large molecular weight nanostructures and then modify them to the electrodes in one step. Nowadays, many DNA nanostructure, such as tetrahedral,[29] dendritic,[24] wireframe,[30] DNA origami,[31] have been developed for sensing or drug delivery. Therefore, the one-step approach of introducing high molecular weight DNA nanostructures to electrodes can avoid the

cumbersome steps of gradually modifying the low molecular weight nucleic acid, possessed high universality and easy to operate, which will be a subject worthy to investigate.

In the last decades, the analytical application of ECL is mainly focused on $Ru(bpy)_3^{2+}$, luminol and their derivatives.[32] In order to enrich the application of ECL, many efforts have been devoted to developing novel nanomaterial-based ECL systems including carbon dots,[33] novel quantum dots,[34] metal nanoclusters.[35] Not long ago, terbium organic gels (TOGs) was reported as promising ECL emitters for the first time because of their advantages of easy preparation, long lifetime and strong ECL emission.[36] As a rising star in ECL fields, it is meaningful to expand its analytical application, especially in the field of nucleic acid detection.

With these in mind, we constructed a novel ECL biosensor based on a target-triggered cascade branched hybridization chain reaction (bHCR) circuit to fill the vacancy of bioanalytical application of TOGs. Our work combined DNA nanotechnology with a highly simple and credible one-step modification strategy. The novel two-layered concatenated HCR-1 circuit and HCR-2 circuit with synergistic amplification performance (scheme 1A). This integrated biosensor not only can achieve double circulation amplification of nucleic acid, but possessed the advantage of being extremely easy to operate, improved the reliability, and achieved ultrasensitive detection. As exhibited in Scheme 1, TOGs-Au NPs films on the GCE electrode were used as a

detection platform which can perform strong ECL emission. Then, the abundant dopamine (DA) introduced by nucleic acid amplification technology was utilized to quench the ECL signal of TOGs. In the branched chain reaction circuit, low molecular weight target microRNA-141 (miRNA-141) performing as the input sequence could trigger the programmed self-assembly of DA-labelled hairpin DNA to obtain high molecular weight hyper-branched DNA structure, which was then introduced into the electrode by a one-step method, resulting in the significantly quenched ECL signal of TOGs. This work offers new emerging TOGs as the ECL emitters, gets efficient quenching improvement, and more importantly, hopes that the one-step introducing DNA strategy can remind everyone to pay attention to minimize the systematic error when constructing electrochemical biosensors.

Scheme 1. (A) The dual signal amplification bHCR strategy triggered by miRNA-141. (B) The fabrication process of the biosensor based on the one-step introduction approach.

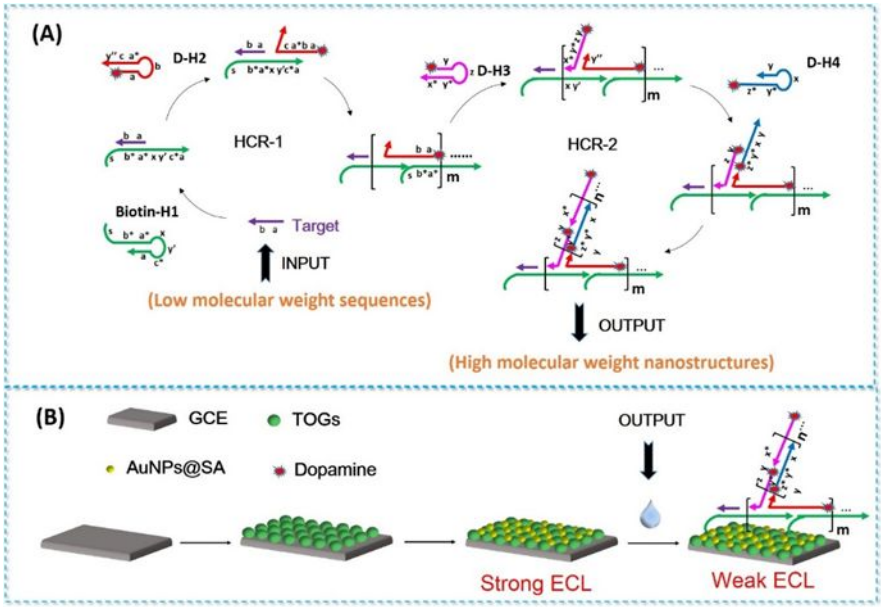

EXPERIMENTAL SECTION

Reagents and materials. The chemicals and reagents in this work were of analytical grade and were used directly without further purification. 4'-(4-carboxyphenyl)-2, 2':6', 2''-terpyridine (Hcptpy) (97%) was obtained from Shanghai UCHEN Ink (Shanghai, China). Terbium nitrate pentahydrate ($Tb(NO_3)_3$), potassium persulfate ($K_2S_2O_8$) were purchased from Aladdin Co., Ltd (Shanghai, China). Bovine serum albumin (BSA) was obtained from Dingguo Changsheng Biotechnology Co., Ltd. (Beijing, China). 30 nm Au NPs were purchased from Hualan Chemical Technology Co., Ltd. (Shanghai, China). N-Ethyl-N'-(3-dimethylaminopropyl) carbodiimide hydrochloride (EDC), N-hydroxysulfosuccinimide (NHS), streptavidin (SA), and tris(2-carboxyethyl) phosphine

(TCEP) were purchased from Sigma-Aldrich Chemicals Co. (Shanghai, China). The ethidium bromide stock solution (EB, 10 mg/mL) and the oligonucleotides were all obtained from the Sangon Biotech Co., Ltd. (Shanghai, China).

Apparatus. MPI-E ECL Analyzer (Xi'an Remex Co. Ltd., China) was used to record the ECL signals. The three-electrode system was used in the electrochemical experiments: bare or modified glass carbon electrodes (GCE, 3 mm diameter) as the working electrodes, a platinum wire as the auxiliary electrode, and an Ag/AgCl (saturated KCl) electrode as the reference electrode. The voltage of the photomultiplier tube (PMT) was 800 V with the scan rate of 0.3 V/s in the process of detection. The CHI 660D electrochemical workstation (CH Instrument Co. Shanghai) was used to carried out the cyclic voltammetry (CV) and electrochemical impedance spectroscopy (EIS) tests. The morphology of the as-prepared TOGs were characterized by scanning electron microscope (SEM, Hitachi S-4800). X-ray photoelectron spectrometry (XPS) analyses were carried out on a Thermo escalab 250 Xi X-ray photoelectron spectrometer. Ultraviolet-visible (UV-vis) absorption spectra and photoluminescence spectra were carried out with the Hitachi U-3010 spectrometer and a Hitachi F-2500 fluorescence spectrophotometer (Tokyo, Japan), respectively.

Preparation of TOGs and streptavidin coated Au NPs. The preparation of TOGs used a simply one-step mixing method, according to previous literature.[36] 200 μL 0.112 M of $Tb(NO_3)_3$ and 200 μL of 0.112 M Hcptpy was mixed completely followed by

resting at room temperature. After that, the synthesized TOGs was treated by centrifugation and washing. Finally, the centrifuged TOGs was dispersed by 800 μL of H_2O. Preparation of streptavidin coated Au NPs by minor modification according to a previously reported procedure.[37] Briefly, the 30 nm Au NPs were first adjusted to pH 6.4 with $K_2C_2O_3$. Then, 100 μL of 2 mg/mL streptavidin was mixed with 1 mL of Au NPs incubated for 30 minutes. Next, the conjugated SA-Au NPs were treated with centrifugation to obtain the red precipitates. Finally, 1×PBS solution containing 1% BSA was used to disperse the red precipitates.

Preparation of DA labeled hairpin DNA. In this work, obtained hairpin DNA (H2, H3, H4) have been modified with carboxyl groups firstly. Cross-linking of ECL quenching reagent DA (–NH2) and H2 (-COOH) was received employing EDC and NHS by the following steps referring to related literature.[38] In short, 50 μL of 5 μM H2 (-COOH) was activated through 15 μL of EDC (1.5 M) and 15 μL of NHS (0.35 M) for 3 h. Next, 20 μL of DA (0.1 M) was injected into the activated H2 solution and reacted overnight. The result is that, the DA labled H2 (D-H2) signal probes was obtained. Similarly, DA labeled H3 (D-H3) and DA labeled H4 (D-H4) were synthesized by the procedure above but replacing H2 with H3 or H4.

Preparation of bHCR circuit. The mechanistic illustration of bHCR circuit was shown in Scheme 1A. The bHCR circuit strategy in this work depends on the layered coupling design of upstream HCR-1 and downstream transducer HCR-2. All the DNA

hairpins need to be annealed prior to use, heated for 3 min at 95℃ and slowly cooled to 25 ℃. Interestingly, miRNA-141 acts as a trigger sequence that triggers the operation of the DNA circuit, since miRNA-141 can open the neck of H1 and then trigger the subsequent hairpins for self-assembly. For the sensitive detection of miRNA-141 by proposed amplification method, different concentrations of miRNA-141 were introduced into the mixture of H1 (1 μM), D-H2 (1 μM), D-H3 (1 μM), D-H4 (1 μM) to trigger the circuit operating spontaneously like a molecular machine at 37℃ for 6h.

Native polyacrylamide gel (PAGE) electrophoresis. 500 nM of miRNA-141 was incubated with 1 μM of the corresponding hairpin mixtures in reaction buffer for 6 h. After mixing different samples with the loading buffer, carefully added them to the lanes of the gel electrophoresis (see SI for the preparation process), respectively. After running at 100 V for about 100 min, the gel was stained in EB solution for 15 min. Finally, the electrophoresis photo after staining was obtained by photographing under UV light.

Construction of the biosensor and analysis procedure. First, the glassy carbon electrode (GCE) was polished and washed to make the surface of the electrode mirror-like. Thereafter, 5 μL of TOGs and 5 μL of Au NPs solutions was dropped onto the pretreated electrodes surface and dried naturally in the air, respectively. Next, 8 μL of bHCR circuit solutions was dripped onto the surface of the electrode for 6 h, then the branched chain reaction circuit was linked to the electrode surface through the specific binding of streptavidin and biotin. After washing with PBS, the constructed biosensor

was detected in buffer solution (0.1 M, pH 7.4) containing 10 mM $K_2S_2O_8$ from 0 to -2 V.

RESULTS AND DISCUSSION

Characterization of as-prepared TOGs. SEM characterization was employed to observe the morphology of TOGs. As depicted in Figure S1, the SEM image showed the uniform particle shape of the gel of approximately 50 nm. Rheological tests were carried out to comprehend the mechanical property of this gels. Dynamic frequency sweep (Figure 1A) revealed that the elasticity (G') and viscosity (G'') were about 125 and 25 Pa, respectively. G' and G'' showed weak frequency dependence in the frequency range from 0.1 to 100 rad s^{-1}, and the G' was larger than its corresponding G'', indicating that a real gel material was formed. UV-vis and fluorescence measurements were carried out to survey optical properties of TOGs. As shown in Figure 1B, the main ultraviolet absorption peak at about 282 nm was ascribe to the typical $\pi \rightarrow \pi^*$ transition of C=C. The emission bands at 492 and 546 nm were attributed to the $^5D_4 \rightarrow {}^7F_6$ and $^5D_4 \rightarrow {}^7F_5$ transition of terbium, respectively. In addition, the eye-visible green fluorescence from inverted TOGs was observed under 365 nm ultraviolet (UV) lamp (Figure 1B, insert). Furthermore, X-ray photoelectron spectroscopy (XPS) was utilized to understand the chemical composition of TOGs, the result was shown as Figure S2. The peaks at 285.6, 401,532, 1276.4, and 1241.9 eV were attributed to C 1s, N 1s, O 1s, Tb $3d_{3/2}$ and $3d_{5/2}$,

respectively, suggesting that these elements exist in TOGs. These results above indicated the successful synthesis of TOGs material.

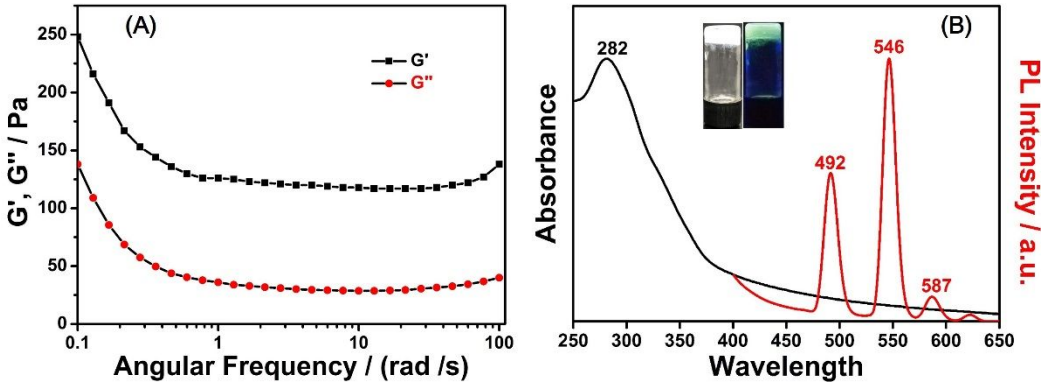

Figure 1. (A) Variation of elasticity (G') and viscosity (G'') with frequency for TOGs, strain = 3%. (B) UV-vis absorption (black line) and PL spectra (red line) of TOGs. Insert: photo of TOGs illuminated by natural light (left) and ultraviolet (right).

Feasibility of the branched chain reaction circuit. To assess the feasibility of the branched hybridization chain reaction circuit, the prepared samples of different controlled experiments were first carried out by PAGE experiment. To verify whether the bHCR circuit operated as expected, each layer of the bHCR circuit, including upstream HCR-1 and downstream HCR-2, were confirmed through PAGE separately. As shown in Figure 2A of the gel electrophoresis photo, it is obviously observed that Lane 2 (T1:H1:H2) and Lane 3 (T2:H3:H4) possessed a much lower migration rate than single strands in Lane 7 (H1), Lane 8 (H2), Lane 9 (H3) and Lane 10 (H4). The results verified that H1 and H2 assembly into HCR-1 or H3 and H4 assembly into HCR-2 are triggered by the trigger

nucleic acid sequence (T1, that is, miRNA-141) or secondary initiator sequence (T2), respectively. Compared with Lane 3 and Lane 4, we can easily see that there is a faint band on the upper part of lane 4, indicating that the addition of H3 can form a larger DNA structure. Compared with Lane 5 (T1:H1:H2:H3:H4) and Lane 6 (H1:H2:H3:H4), a brighter band appeared at the top of Lane 5, and the color of raw DNA band at the bottom significantly reduced. However, no obvious band appeared at the top of Lane 6, indicating that this bHCR circuit can be effectively triggered only in the presence of miRNA-141. Overall, the designed bilayer nucleic acid circuit operated as expected: in the absence of target miRNA-141, the reaction speed was extremely slow (Lane 6), but only a small number of target sequence can promote the circuit to operate rapidly to near reaction completeness (Lane 5). To further confirm this bHCR system can indeed form the desired branched DNA nanostructures, TEM characterization was carried out trying to directly see the morphology of the product obtained after the self-assembly reaction. As Figure 2B and 2C intuitively shown, the branched DNA structure was discovered in the bHCR system after incubation of target miRNA-141 with H1, H2, H3, and H4, validating the proposed bHCR design.

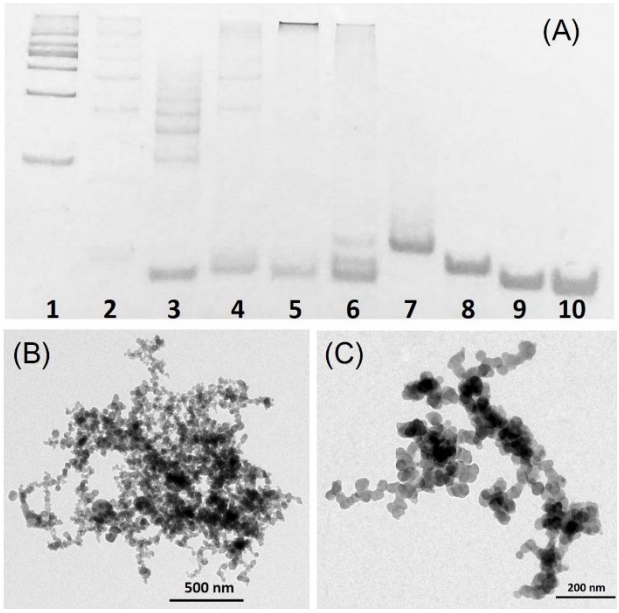

Figure 2. (A) PAGE (12%) analysis of the DNA hyperbranched circuit. Lane 1: DNA ladder marker; Lane 2: T1 (250 nM) + H1 (500 nM) + H2 (500 nM); Lane 3: T2 (500 nM) + H3 (1μM) + H4 (1μM); Lane 4: T1 (250 nM) + H1 (500 nM) + H2 (500 nM) + H3 (1μM); Lane 5: T1 (250 nM) + H1 (500 nM) + H2 (500 nM) H3 (1μM) + H4 (1μM); Lane 6: H1 (500 nM) + H2 (500 nM) + H3 (1μM) + H4 (1μM); Lane 7: H1 (1 μM); Lane 8: H2 (1 μM); Lane 9: H3 (1 μM); Lane 10: H4 (1 μM). (B) TEM images of the assembly products. Part (C) is enlarged details of part (B).

ECL mechanism of the biosensor. Innovative luminophore is a key factor in enhancing the ECL signal. TOGs was employed as the efficient ECL emitter to detect nucleic acid for the first time. When the scanning potential was sufficiently negative and in the presence of the $K_2S_2O_8$, TOGs and $S_2O_8^{2-}$ could be reduced to form $TOGs^{\bullet-}$ and $SO_4^{\bullet-}$, then the strong oxidant $SO_4^{\bullet-}$ can react with the reducing agent $TOGs^{\bullet-}$ to generate the

excited-stated TOG*, producing an enhanced ECL signal. Dopamine (DA), a neurotransmitter within the brain link to various diseases of disease, was considered as the universal ECL quencher ascribed to that the strong oxidant $SO_4^{\bullet-}$ could oxidize DA to o-benzoquinone species which can accept energy from the excited of TOGs.[39,40]

In order to confirm that DA can quench the ECL signal of TOGs, we conducted the following experiments. First, the amount of TOGs used to modify the GCE was optimized. Figure 3A displayed the influence of the amount of TOGs on the ECL intensity. As the concentration of TOGs increased from 0 to 1 mg/ml, the ECL intensity gradually increased. The maximum is reached at 1 mg/ml and then decreased, which may ascribed to that too much TOGs on the surface of GCE will block the electron transfer. Thus, the concentration of TOG selected for use in this experiment was 1 mg/mL. After that, the proposed TOGs-$K_2S_2O_8$ ECL system was used to detect different concentration of dopamine. As Figure 3B shows, in the concentration range of 0 to 1000 pM, the ECL intensity decreased markedly as the concentration of DA increased. These results illustrated that DA can significantly quench the ECL of TOGs. Thus, the DA-modified DNA sequence can be applied to construct DNA cycling to switch off the ECL signal. As shown in Scheme 1, when the target was input in the circuit, target as the initiator can open the hairpin structure of H1 and leak out the sequence that can open the H2 hairpin structure. Interestingly, the opened H2 hairpin can leak out the sequence that can trigger the HCR-2 to form the hyperbranched DNA nanostructures. However, in the absence of

target, these hairpin sequences can't hybridize each other because there is no toehold sequence to open these hairpins. That is, only using the target as the trigger, the double amplification cycles can be achieved under isothermal conditions, resulting in the DNA structure with numerous dopamine molecules. Moreover, the TOGs/AuNPs was constructed as the novel sensing platform. The obtained DNA nanostructure can be introduced to the surface of GCE due to the specific reaction of SA (SA@Au NPs) and biotin (biotin-H1). Finally, the sensitivity of the biosensor can be assessed by changes of the ECL signal value as changes of the target concentration. With our method, DNA can be introduced into to electrode surface in one step, eliminating the need for layer-by-layer assembly, which greatly simplifies the procedure and reduces the error to some extent.

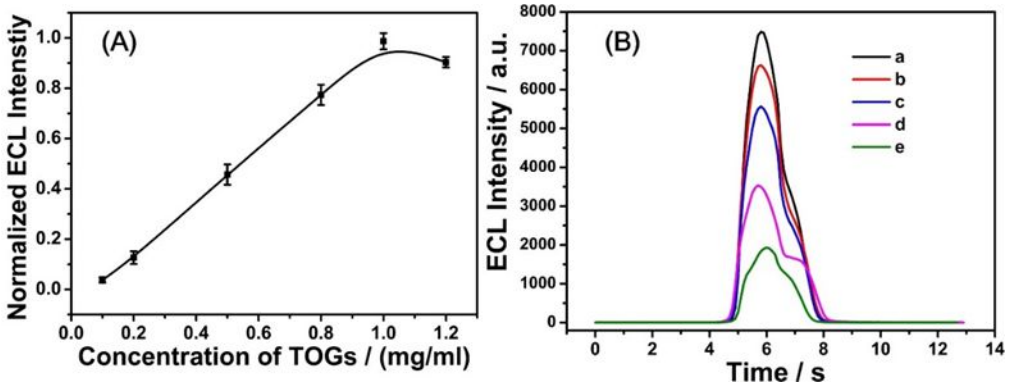

Figure 3. (A) Effect of the concentration of TOGs on ECL intensity. (B) ECL curves for TOGs/GCE in pH 7.4 PBS solution containing different concentration of DA (from a to e: 0, 1 pM, 10 pM, 100 pM, 1000 pM).

Characterization of the biosensor. First, we characterized the morphology of the electrodes. As shown in Figure S3A, a disordered densely network of TOGs on the surface of GCE was observed. When Au NPs were added to the TOGs modified GCE (Figure S3B), many bright particles could be seen on the SEM image, and the surface of the electrode exhibited the color of slight purple, indicating that the Au NPs/TOGs/GCE was successfully constructed and could provide a good platform for the subsequent one-step introduction of DNA nanostructure. Electrochemical Impedance Spectroscopy (EIS) as a facile electrochemical technique can be used to monitor the assembly process based on the electron-transfer resistance (R_{et}). As shown in Figure S4, GCE has less R_{et} than TOGs/GCE which was mainly due to the poor conductivity of TOGs. After depositing Au NPs on the TOGs/GCE electrode surface, the R_{et} was significantly reduced since Au NPs acted as the good conductor to promote electron transfer. However, when the DNA solution was added to the electrode, the resistance R_{et} increased obviously due to the increase of steric hindrance and the reduction of electron transfer efficiency. These characterization suggested our biosensor was successfully fabricated.

Detection of miRNA-141 with the developed biosensor. On the basis of the target-triggered branched chain reaction circuit coupled with the novel ECL emitter, we can apply this ECL biosensor sensitively detect microRNAs. First, the reproducibility of the ECL biosensor was evaluated by continuous cyclic potential scanning for 15 cycles. Through experiment, a relative standard deviation (RSD) of 2.4% was achieved (Figure

4A), indicating acceptable reproducibility of the developed biosensor. It has been reported that miRNA-141 overexpressed in prostate cancer (22 Rv1 cell line), thus miRNA-141 can be employed as cancer biomarkers for early diagnosis of prostate cancer.[41] To explore the possible application of the one-step introduction DNA nanostructure ECL biosensor, various concentration of miRNA-141 were employed as the initiator to form the hyperbranched DNA nanostructures. As depicted in Figure 4B, the ECL intensity gradually decreased when increasing the concentration of miRNA-141. As shown in Figure 4C, the ECL signal followed a good linear trend over the logarithmically concentration of miRNA-141 ranging from 0.5 fM to 500 fM (R^2 = 0.995). The obtained linear regression equation was $y = 6462.23 – 2028.04\ x$ (y refers the ECL intensity, and x refers to the logarithmical-concentration of miRNA-141), and the limit of detection (LOD) was 0.18 fM. Compared with some recently reported miRNA-141 detection methods (Table S2), our proposed method of introducing target-triggered branched chain reaction circuit to the electrode in one step possessed lower LOD than those of assays mentioned, including colorimetric, fluorescence, electrochemistry, and other methods.

Further, the selectively of the biosensor was investigated. Three different non-complementary oligonucleotides including miRNA-155, miRNA-21, miRNA-199a, and the single-base mismatched, double-base mismatched oligonucleotides were tested. As shown in Figure 4D, significant weak ECL was obtained when miRNA-141 was used as

the target, while ECL signal did not change obviously when other microRNAs were used as target. These results suggested that the high specificity of the target-triggered bHCR circuit strategy for miRNA-141 detection.

To assess the feasibility of the proposed ECL biosensor for clinical application, the standard addition method was applied to the spiked healthy human serum. Serum samples with a spiked concentration of 10 fM and 100 fM miRNA-141 were mixed with other hairpin DNAs (including biotin-H1, D-H2, D-H3, and D-H4) to form the DNA nanostructure, which were introduced to the electrode after that. Then the ECL signal responses from the spiked samples were recorded and the measured concentration were calculated by the linear equation. The results were shown in Table S3, the recovery of spiked miRNA-141 was between 91% and 106%, suggesting that the proposed ECL biosensor had potential applications in clinical analysis.

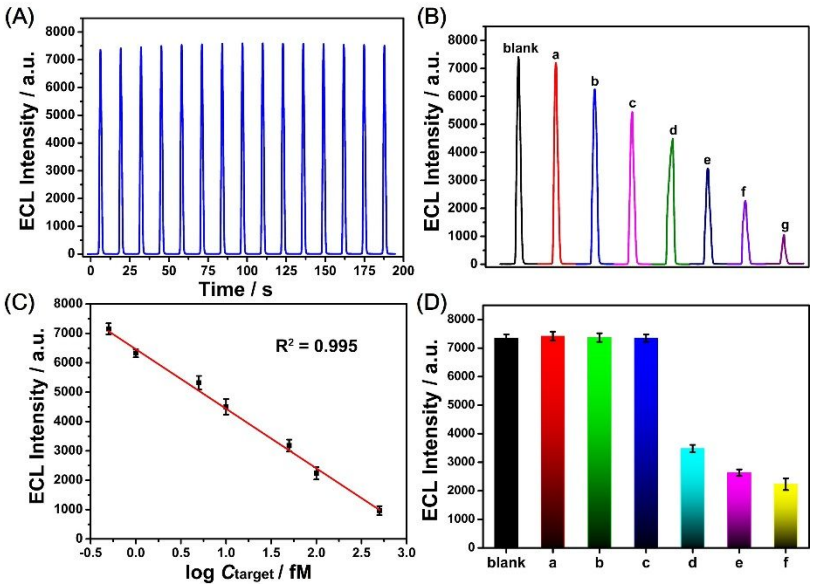

Figure 4. (A) The stability of the biosensor. (B) ECL response of the biosensor to miRNA-141 with different concentration: (a-g) 0.5, 1, 5, 10, 50, 100, 500 fM. (C) The calibration curve for miRNA-141. (D) Selectivity of the ECL biosensor incubated in blank, miRNA-155 (a), miRNA-21 (b), miRNA-199a (c), single-base mismatched (d), double-base mismatched oligonucleotides (e), miRNA-141 (f).

CONCLUSIONS

In summary, we have developed a biosensor for detection of miRNA based on the bHCR circuit that integrated the novel ECL emitter TOGs. On the one hand, as a novel ECL matrix, the TOGs/Au NPs could provide superior ECL signal. On the other hand, the enzyme-free nucleic acid bHCR circuit amplification was propitious to the improvement of sensitivity, exhibiting outstanding amplification capacity and specificity. Unlike the traditional stepwise modification nucleic acids to the electrode, the novel one-step approach of introduction of DNA nanostructures into the electrodes offers both high sensitivity and credibility. The proposed ECL biosensor demonstrated good accuracy, facile and green treatments in the detection of nucleic acids using miRNA-141 as the model analyte. This work would greatly pave the way for studying less explored on simple modification of nucleic acid structures into electrode with competitive performances.

ASSOCIATED CONTENT

Supporting Information

The Supporting Information is available free of charge on the ACS Publications website. Reagents and materials; apparatus; preparation of PAGE; oligonucleotide sequences; SEM and XPS of TOGs; SEM image of TOGs and AuNPs/TOGs modified GCE; EIS spectra of the GCE at different stages; comparison for the existing methods; real blood sample analysis. (PDF)

AUTHOR INFORMATION

Corresponding Author

*** E-mail:** chengzhi@swu.edu.cn

*** E-mail:** liyf@swu.edu.cn

ORCID

Cheng Zhi Huang: 0000-0002-1260-5934

Yuan Fang Li: 0000-0001-5710-4423

Notes

The authors declare no competing financial interest.

ACKNOWLEDGMENT

This work was financially supported by the National Natural Science Foundation of China (NSFC, No. 21575117).

REFERENCES

(1) Bartel, D. P. *Cell* **2009**, *136*, 215-233.

(2) Baek, D.; Villén, J.; Shin, C.; Camargo, F. D.; Gygi, S. P.; Bartel, D. P. *Nature* **2008**, *455*, 64-71.

(3) Bartel, D. P. *Cell* **2004**, *116*, 281-297.

(4) Li, M.; He, Y.; Zhou, Z.; Ramirez, T.; Gao, Y.; Gao, Y.; Ross, R. A.; Cao, H.; Cai, Y.; Xu, M.; Feng, D.; Zhang, P.; Liangpunsakul, S.; Gao, B. *Gut* **2017**, *66*, 705-715.

(5) Gu, Y.; Song, J.; Li, M.-X.; Zhang, T.-T.; Zhao, W.; Xu, J.-J.; Liu, M.; Chen, H.-Y. *Anal. Chem.* **2017**, *89*, 10585-10591.

(6) Smith, L.; Kohli, M.; Smith, A. M. *J. Am. Chem. Soc.* **2018**, *140*, 13904-13912.

(7) Xia, Y.; Wang, L.; Li, J.; Chen, X.; Lan, J.; Yan, A.; Lei, Y.; Yang, S.; Yang, H.; Chen, J. *Anal. Chem.* **2018**, *90*, 8969-8976.

(8) Hosseinzadeh, E.; Ravan, H.; Mohammadi, A.; Mohammad-rezaei, R.; Norouzi, A.; Hosseinzadeh, H. *Biosens. Bioelectron.* **2018**, *117*, 567-574.

(9) Xu, L.; Gao, Y.; Kuang, H.; Liz-Marzán, L. M.; Xu, C. *Angew. Chem. Int. Ed.* **2018**, *57*, 10544-10548.

(10) Miao, P.; Jiang, Y.; Zhang, T.; Huang, Y.; Tang, Y. *Chem. Commun.* **2018**, *54*, 7366-7369.

(11) Yu, S.; Wang, Y.; Jiang, L.-P.; Bi, S.; Zhu, J.-J. *Anal. Chem.* **2018**, *90*, 4544-4551.

(12) Zhou, Y.; Wang, H.; Zhang, H.; Chai, Y.; Yuan, R. *Anal. Chem.* **2018**, *90*, 3543-3549.

(13) Liu, Q.; Ma, C.; Liu, X.-P.; Wei, Y.-P.; Mao, C.-J.; Zhu, J.-J. *Biosens. Bioelectron.* **2017**, *92*, 273-279.

(14) Miao, W. *Chem. Rev.* **2008**, *108*, 2506-2553.

(15) Yao, Q.; Wang, Y.; Wang, J.; Chen, S.; Liu, H.; Jiang, Z.; Zhang, X.; Liu, S.; Yuan, Q.; Zhou, X. *ACS Nano* **2018**, *12*, 6777-6783.

(16) Ren, K.; Xu, Y.; Liu, Y.; Yang, M.; Ju, H. *ACS Nano* **2018**, *12*, 263-271.

(17) Wang, H.; Li, C.; Liu, X.; Zhou, X.; Wang, F. *Chem. Sci.* **2018**, *9*, 5842-5849.

(18) Deng, L.; Wu, Y.; Xu, S.; Tang, Y.; Zhang, X.; Wu, P. *ACS Sens.* **2018**, *3*, 1190-1195.

(19) Chi, J.; Shao, C.; Du, X.; Liu, H.; Gu, Z. *ACS Appl. Mater. Interfaces* **2018**, *10*, 39144-39150.

(20) Jiang, X.; Loeb, J. C.; Manzanas, C.; Lednicky, J. A.; Fan, Z. H. *Angew. Chem. Int. Ed.* **2018**, *57*, 17211-17214.

(21) Wang, J.; Pan, M.; Wei, J.; Liu, X.; Wang, F. *Chem. Commun.* **2017**, *53*, 12878-12881.

(22) Bi, S.; Yue, S.; Zhang, S. *Chem. Soc. Rev.* **2017**, *46*, 4281-4298.

(23) Wei, J.; Gong, X.; Wang, Q.; Pan, M.; Liu, X.; Liu, J.; Xia, F.; Wang, F. *Chem. Sci.* **2018**, *9*, 52-61.

(24) Xuan, F.; Hsing, I. M. *J. Am. Chem. Soc.* **2014**, *136*, 9810-9813.

(25) Yin, P.; Choi, H. M. T.; Calvert, C. R.; Pierce, N. A. *Nature* **2008**, *451*, 318-322.

(26) Wu, Y.; Zhang, D. Y.; Yin, P.; Vollmer, F. *Small* **2014**, *10*, 2067-2076.

(27) Nie, Y.; Yuan, X.; Zhang, P.; Chai, Y.-Q.; Yuan, R. *Anal. Chem.* **2019**, *91*, 3452-3458.

(28) Huang, R.; He, N.; Li, Z. *Biosens. Bioelectron.* **2018**, *109*, 27-34.

(29) Ma, J.; Xue, L.; Zhang, M.; Li, C.; Xiang, Y.; Liu, P.; Li, G. *Biosens. Bioelectron.* **2019**, *127*, 194-199.

(30) Hoffecker, I. T.; Chen, S.; Gådin, A.; Bosco, A.; Teixeira, A. I.; Högberg, B. *Small* **2019**, *15*, 1803628.

(31) Huang, Y.; Nguyen, M.-K.; Natarajan, A. K.; Nguyen, V. H.; Kuzyk, A. *ACS Appl. Mater. Interfaces* **2018**, *10*, 44221-44225.

(32) Mayer, M.; Takegami, S.; Neumeier, M.; Rink, S.; Jacobi von Wangelin, A.; Schulte, S.; Vollmer, M.; Griesbeck, A. G.; Duerkop, A.; Baeumner, A. J. *Angew. Chem. Int. Ed.* **2018**, *57*, 408-411.

(33) Long, Y.-M.; Bao, L.; Peng, Y.; Zhang, Z.-L.; Pang, D.-W. *Carbon* **2018**, *129*, 168-174.

(34) Wang, H.; Pu, G.; Devaramani, S.; Wang, Y.; Yang, Z.; Li, L.; Ma, X.; Lu, X. *Anal. Chem.* **2018**, *90*, 4871-4877.

(35) Zhai, Q.; Xing, H.; Zhang, X.; Li, J.; Wang, E. *Anal. Chem.* **2017**, *89*, 7788-7794.

(36) Li, Y.; Jiang, Z. W.; Xiao, S. Y.; Huang, C. Z.; Li, Y. F. *Anal. Chem.* **2018**, *90*, 12191-12197.

(37) Niu, Y.; Zhao, Y.; Fan, A. *Anal. Chem.* **2011**, *83*, 7500-7506.

(38) Zhang, P.; Wu, X.; Yuan, R.; Chai, Y. *Anal. Chem.* **2015**, *87*, 3202-3207.

(39) Liu, X.; Jiang, H.; Lei, J.; Ju, H. *Anal. Chem.* **2007**, *79*, 8055-8060.

(40) Peng, H.; Liu, P.; Wu, W.; Chen, W.; Meng, X.; Lin, X.; Liu, A. *Anal. Chim. Acta* **2019**, *1065*, 21-28.

(41) Calin, G. A.; Croce, C. M. *Nat. Rev. Cancer* **2006**, *6*, 857-866.

For TOC only

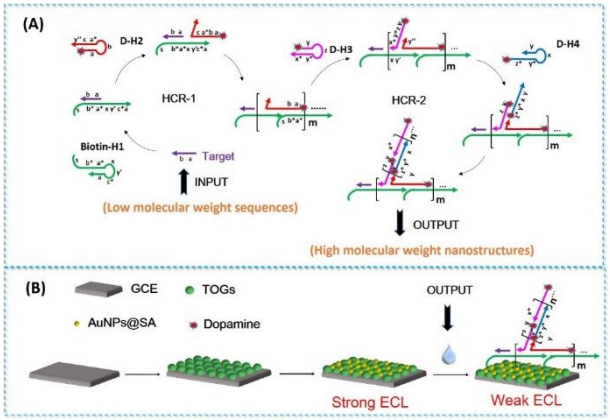
(A)
D-H2
D-H3
D-H4
HCR-1
HCR-2
Biotin-H1
Target
INPUT
(Low molecular weight sequences)
OUTPUT
(High molecular weight nanostructures)
(B)
GCE
TOGs
AuNPs@SA
Dopamine
OUTPUT
Strong ECL
Weak ECL